A NEW SOLUTION FOR SHALLOW AND DEEP TUNNELS BY CONSIDERING THE GRAVITATIONAL LOADS

MOHAMMAD REZA ZAREIFARD and AHMAD FAHIMIFAR

about the authors

Mohammad Reza Zareifard
Amirkabir University of Technology
Tehran, Iran
E-mail: zareefard@aut.ac.ir

corresponding author

Ahmad Fahimifar
Amirkabir University of Technology
Tehran, Iran
E-mail: fahim@aut.ac.ir

Abstract

A new, elasto-plastic, analytical-numerical solution, considering the axial-symmetry condition, for a circular tunnel excavated in a strain-softening and Hoek–Brown rock mass is proposed. To examine the effect of initial stress variations, and also the boundary conditions at the ground surface, the formulations are derived for different directions around the tunnel. Furthermore, the effect of the weight of the plastic zone is taken into account in this regard. As the derived differential equations have no explicit analytical solutions for the plastic zone, the finite-difference method (FDM) is used in this study. On the other hand, analytical expressions are derived for the elastic zone. Several illustrative examples are given to demonstrate the performance of the proposed solution, and to examine the effect of various boundary conditions. It is concluded that the classic solutions, based on the hydrostatic far-field stress, and neglecting the effect of the boundary conditions at the ground surface, give applicable results for a wide range of practical problems. However, ignoring the weight of the plastic zone in the analyses can lead to large errors in the calculations.

keywords

ground-response curve, elasto-plastic analysis, boundary condition, axial symmetry, gravitational loads

1 INTRODUCTION

A number of methods are currently used for the design and analysis of tunnels. Among them, the convergence-confinement method (the C.-C. method) has played an important role in providing an insight into the interaction between the lining support and the surrounding ground mass. The C.-C. method is based on a concept that involves an analysis of the ground-structure interaction by independent studies of the behavior of the ground and of the tunnel support. In this regard, the ground behavior is represented by a ground-response curve; which describes the ground convergence in terms of the applied internal pressure. However, to maintain simplicity, a number of simplifying assumptions are made in its derivation. These assumptions make the method applicable only to deep tunnels in hydrostatic stress fields. In the past, a number of classic solutions for determining the ground-response curve have been published. These solutions may be categorized into two groups of analytical closed-form solutions and analytical-numerical unclosed-form solutions. Although a number of closed-form solutions are available (such as that proposed by Brown et al. [1]; Sharan [2]; Carranza-Torres [3]; Park and Kim [4]), each solution suffers from a level of approximation in the sense that it incorporates various simplifying assumptions. For example, these solutions have been proposed for the rock masses with simpler behavior models, including the elastic-perfect-plastic or elastic-brittle-plastic behavior models. In fact, for more complicated behavior models obtaining an exact closed-form solution is impossible. On the other hand, in the unclosed-form solutions (Brown et al., [1]; Guan et al., [5]; Lee and Pietruszczak, [6]; Fahimifar and Zareifard, [7]), consideration of more complicated and general material-behavior models are possible.

However, all the mentioned solutions (both the closed- and unclosed-form solutions) are based on the classic assumptions made in the C.-C. method. Different aspects of the C.-C. method have been investigated by researchers, both analytically and numerically.

With the development of computer codes, numerical analyses have become common methods for the analysis of tunnels. Various cases of analyses, including two-dimensional, three-dimensional and time-dependent behaviors, can be performed using commercial codes. Nevertheless, utilizing numerical methods for investigating the C.-C. method, such as that presented by Carranza-Torres and Fairhurst [8] and that presented by Gonzalez-Nicieza et al. [9], do not easily reveal the actual effects that the simplifying assumptions have on the mechanical response of a tunnel. Therefore, analytical solutions of simpler cases, such as that proposed by Lu et al. [10], Detournay and Fairhurst [11], and Reed [12], can help to realize various aspects of the ground-response curve of tunnels much better.

In the C.-C. method the effects of the boundary conditions at the ground surface are neglected and, also, the variation of the initial stresses (i.e., in-situ stresses) are not taken into account, classically. However, for shallow tunnels, the initial stresses cannot be assumed to be constant over the tunnel section, and thus the assumption of hydrostatic, far-field stresses may not be applicable. On the other hand, in the C.-C. method, the above solutions neglect the weight of the plastic zone developed around the tunnel. However, very few works concerning the effect of gravitational forces acting on the ground have been conducted [13-15]. In fact, gravitational loading differs for various directions around the tunnel periphery, and, for the same internal pressure, convergence of the crown is expected to be larger than that of the walls, because of the weight of the failed material on the top of the tunnel.

In this paper, an unclosed-form analytical solution is presented for the stress and displacement fields around a circular tunnel excavated in an elasto-plastic strain-softening and Hoek–Brown rock material. In this method the effects of boundary conditions at the free surface of the ground, and also the effect of the weight of the plastic zone are taken into account. For this purpose, the formulations are derived for both the horizontal and the vertical directions that are passing through the tunnel center. In addition, the gravitational loadings are considered as radial body forces being applied to the rock mass.

2 ANALYTICAL SOLUTION OF TUNNELS CONSIDERING THE GRAVITATIONAL LOADS

Fig. 1 shows the general case of a tunnel excavated in a homogeneous and isotropic rock mass under an in-situ stress field below a horizontal ground surface.

In general cases the initial stresses in the Cartesian coordinate system are $\sigma_y = \gamma y + p_s$ and $\sigma_x = \sigma_z = K\sigma_y$, where x, y and z are the Cartesian coordinate axes (as shown in Fig. 1), γ is the specific weight of the rock, K is the so-called lateral stress coefficient, and p_s is the uniform vertical stress that is applied to the ground surface from infrastructures or embankments (surcharge load). In cylindrical coordinates (r,θ,z), the stress field around a tunnel (see Fig. 2) has to fulfill the equilibrium equations for each element of the rock mass, as in [16]:

$$\frac{\partial \sigma_{rr}}{\partial r} + \frac{1}{r}\frac{\partial \sigma_{\theta r}}{\partial \theta} - \frac{\sigma_{\theta\theta} - \sigma_{rr}}{r} + F_r = 0 \qquad (1)$$

$$\frac{\partial \sigma_{r\theta}}{\partial r} + \frac{1}{r}\frac{\partial \sigma_{\theta\theta}}{\partial \theta} + \frac{\sigma_{r\theta} + \sigma_{\theta r}}{r} + F_\theta = 0 \qquad (2)$$

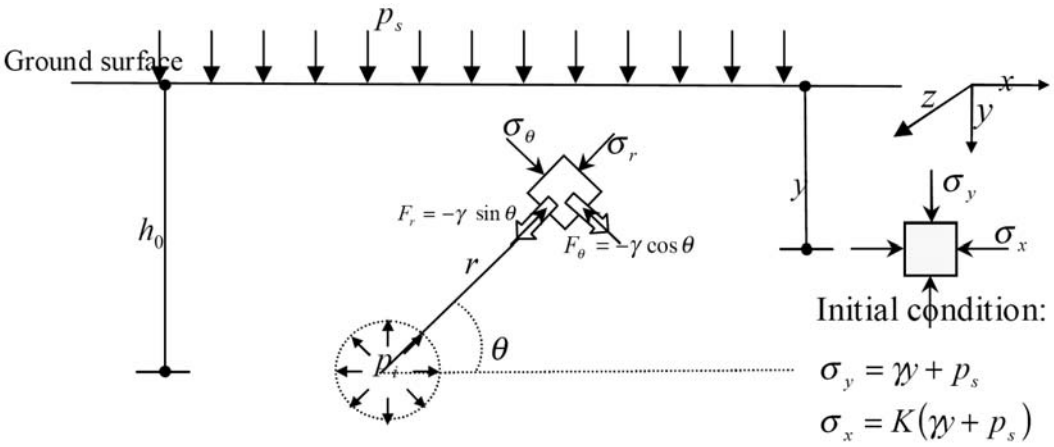

Figure 1. Circular shallow tunnel in a semi-infinite medium under an initial stress field.

where $F_r = -\gamma\sin\theta$, and $F_\theta = -\gamma\cos\theta$ are the gravitational body forces in the radial and circumferential directions, respectively, γ is the unit weight of the ground and θ is the angle measured clockwise from the horizontal direction.

Obtaining an exact elasto-plastic analytical solution for this problem is extremely complicated and even unsolvable in more cases (as shown by Detournay and Fairhurst [11]), because, in this case, the principal stresses may rotate in each direction.

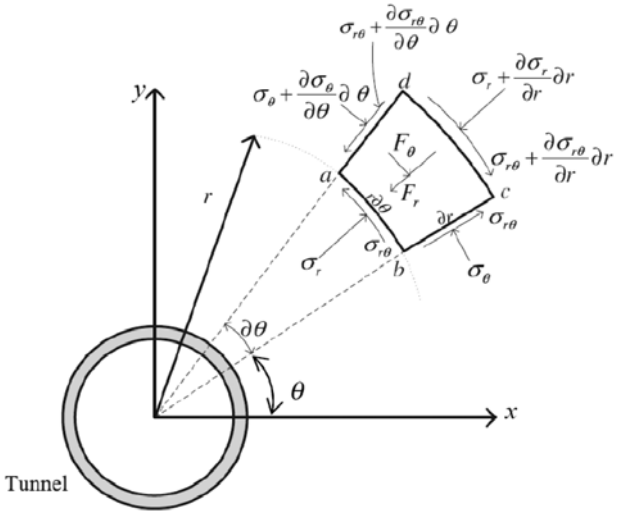

Figure 2. Body forces and stress components corresponding to an element of the rock mass.

As mentioned in the C.-C. method for simplifying the problem, the ground-response curve is constructed based on the elasto-plastic solution for a circular opening subjected to hydrostatic far-field stresses and a uniform internal pressure (see Fig. 3).

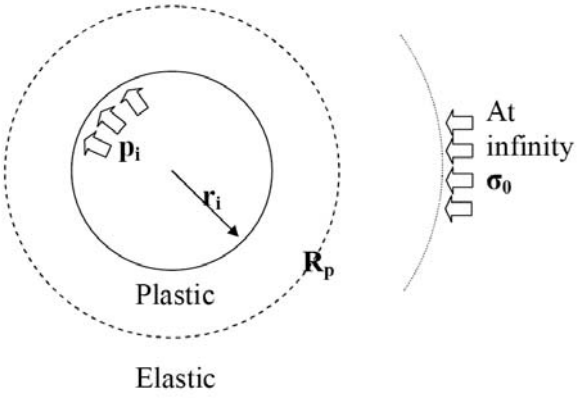

Figure 3. Circular deep tunnel excavated in a hydrostatic stress field.

Thus, in equilibrium Eq. (1) the term $\frac{1}{r}\frac{\partial\sigma_{\theta r}}{\partial\theta}$ vanishes. In this case it is assumed that the initial stresses in the vicinity of the tunnel are constant $\sigma_{y0} = \sigma_{x0} = \gamma h_0 + p_s$ and do not increase linearly.

In this paper an analytical solution for deriving the ground-response curve of a tunnel under equal initial stresses ($K = 1$) is proposed by considering the effects of the initial stress variations due to the gravitational loads and taking the effects of the boundary conditions into account at the free surface of the ground. In this solution the analyses are performed for the horizontal and the vertical directions for axial symmetry conditions (see Fig. 4). Thus, the term $\frac{1}{r}\frac{\partial\sigma_{\theta r}}{\partial\theta}$ will vanishes. In this regard, the governing equilibrium equation becomes more straightforward as:

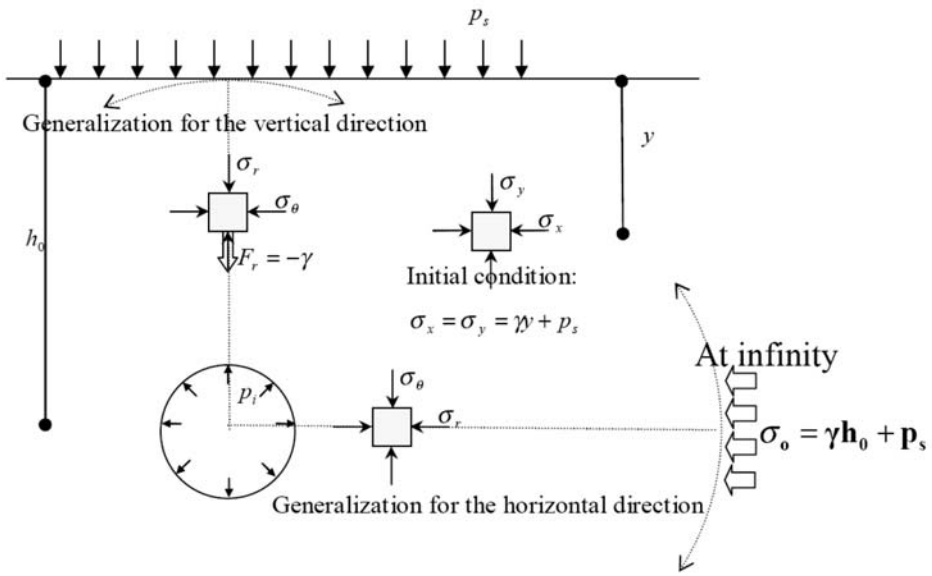

Figure 4. Analysis of the shallow tunnels along the horizontal and the vertical directions by considering the axial symmetry condition.

$$\frac{d\sigma_r}{dr}-\frac{\sigma_\theta-\sigma_r}{r}+F_r=0 \qquad (3)$$

where F_r is the applied radial body force, which depends on the gravitational loads through the considering direction. As mentioned, since the axial symmetry condition is assumed, only the radial component of the gravitational loads, i.e. , $F_r = -\gamma\sin\theta$, is taken into account, and the circumferential component is neglected. Thus, $F_r = -\gamma$ for the vertical direction and $F_r = 0$ for the horizontal direction are obtained (see Fig. 4).

For the polar coordinates defined in Fig. 1, the initial equal stress field ($K = 1$) is given by:

$$\sigma_{0(r,\theta)}=\sigma_{r0(r,\theta)}=\sigma_{\theta 0(r,\theta)}=\gamma y+p_s=\gamma\left(h_0-r\sin\theta\right)+p_s \quad (4)$$

where $\sigma_{\theta 0}$ and σ_{r0} are the initial circumferential and radial stresses, respectively, and p_s is the surcharge load. It should be noted that when there is a very weak or a heavily weathered layer of rock or residual soils on the upper levels, their effect can be considered as surcharge loads applied to the underlying ground.

In this study, the formulations are derived for both the horizontal (through the tunnel springline) and the vertical (through the tunnel crown) directions. In this manner, for both directions, because of the axial symmetry conditions, the geometry, boundary conditions and the applied loads are generalized to all directions (see Fig. 4). The problem for both the horizontal and vertical directions are shown in Figs. 5(a) and 5(b), respectively.

As observed in Figs. 4 and 5(a), for the horizontal direction, the problem is similar to a circular tunnel in an infinite medium. In this case, at the tunnel radius (i.e., at $r = r_i$) the internal pressure p_i is applied, and at an infinite radius (i.e., at $r = \infty$), the pressure $\gamma h_0 + p_s$ is applied. In addition, the radial body forces through this direction are equal to zero. It is observed that this case is similar to the problem of a deep tunnel. On the other hand, as observed in Figs. 4 and 5(b), for the vertical direction, the problem of a thick-walled cylinder is the result. In this case, at the tunnel radius the internal pressure p_i is applied, and at radius $r = h_0$, the pressure p_s is applied. Furthermore, the radial body forces through this direction are $F_r = -\gamma$.

As shown in Fig. 5, two different zones may be formed around the tunnel (for both directions): the external elastic zone, and the internal plastic zone, which may be divided into the softening zone and the residual zone.

The strain–displacement relations in the polar coordinate system for the axial symmetric problem are given by [17]:

$$\varepsilon_\theta=\frac{u_r}{r}, \quad \varepsilon_r=\frac{du_r}{dr} \qquad (5)$$

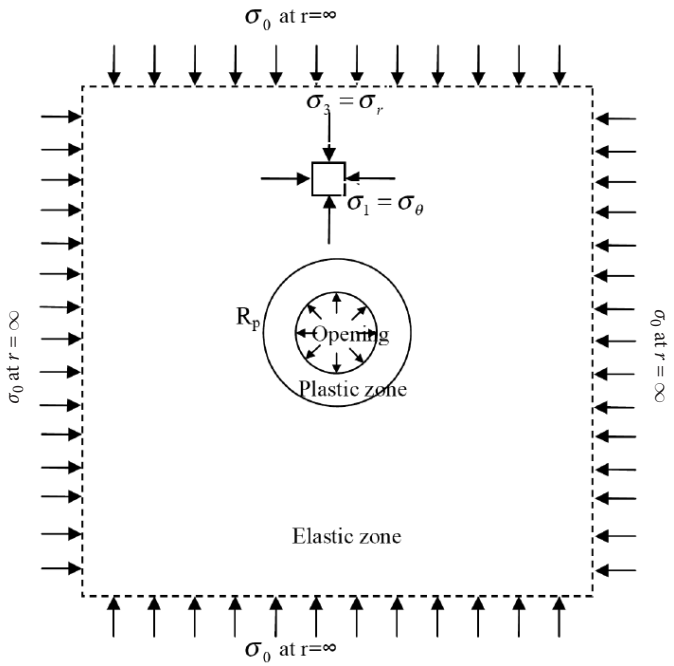

a) Horizontal direction: circular hole in an infinte medium under initial uniform sress $\sigma_0 = \gamma h_0 + p_s$

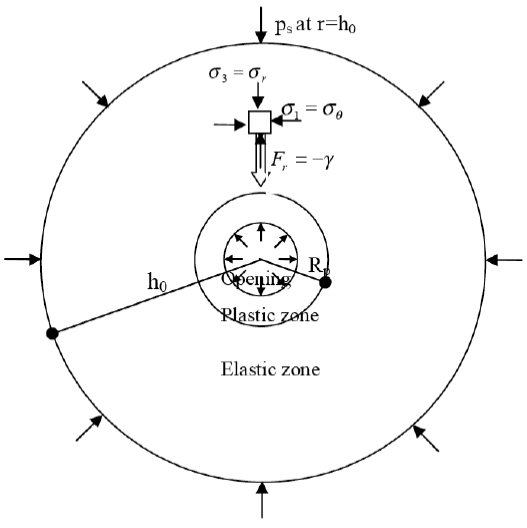

b) Vertical direction: thick walled cylinder under radial gravity loading and a surcharge loading

Figure 5. Geometry, applied loads and boundary conditions for the horizontal and vertical directions.

where u_r is the radial component of the displacement and ε_θ and ε_r are the circumferential and radial strains, respectively.

Furthermore, the stress state at a distance r is defined by the radial stress σ_r and the circumferential stress σ_θ, which are the minor σ_3 and the major σ_1 principal stresses, respectively, as shown in Fig. 5.

3 BEHAVIOR MODEL

The rock mass is assumed to exhibit the strain-softening behavior, in this study, which can be reduced to the perfect elasto-plastic or elasto-brittle-plastic cases. Generally, this behavior is characterized by a transitional failure criterion and a plastic potential. A softening parameter controls the gradual transition from an initial failure criterion (or a potential one) to a residual one. In the present work, the deviatoric plastic strain $\gamma^p = \varepsilon_\theta^p - \varepsilon_r^p$ is employed as the softening parameter. Although there is no universal way of defining the strain-softening parameter, as pointed out by Alonso et al. [18], the above softening parameter is the most widely accepted.

The plastic strain increments can be obtained from the plastic potential function, $g(\sigma_r, \sigma_\theta, \gamma^p)$ according to:

$$\dot{\varepsilon}_r^p = \dot{\lambda}\frac{\partial g}{\partial \sigma_r} \qquad (6)$$

and:

$$\dot{\varepsilon}_\theta^p = \dot{\lambda}\frac{\partial g}{\partial \sigma_\theta} \qquad (7)$$

where $\dot{\lambda}$ is a plastic multiplier, $\dot{\varepsilon}_r^p = \frac{\partial \varepsilon_r^p}{\partial \tau}$ and $\dot{\varepsilon}_\theta^p = \frac{\partial \varepsilon_\theta^p}{\partial \tau}$ (τ is a fictitious 'time' variable). Equations (6) and (7) are the constitutive equations in the plastic regime, and are usually termed the flow rule. If the plastic potential coincides with the failure criterion, then it is called an associated flow rule; otherwise it is called a non-associated flow rule. In this regard the incremental plasticity involves a consideration of a fictitious 'time' variable, even if it does not have any physical meaning. This variable controls the evolution of the plasticity and the plastic strain rates. In the formulation presented in this research, the plastic radius, R_p, will be assumed to be the time variable. This choice allows the acquisition of a simple formulation for the problem, in order to obtain a certain kind of solution, as illustrated by Alonso et al. [18].

Here, the Mohr–Coulomb criterion is selected as a plastic potential function for a non-associated flow rule:

$$g = \sigma_\theta - K_\Psi \sigma_r \qquad (8)$$

where K_ψ is the dilation factor, and is given as:

$$K_\Psi = \frac{1+\sin\Psi_g}{1-\sin\Psi_g} \qquad (9)$$

ψ_g, in Eq. (9), is termed the dilation angle and varies as a function of the softening parameter γ^p.

The rock mass is assumed to obey the Hoek–Brown failure criterion, given by [19]:

$$\sigma_\theta - \sigma_r = \left(m\sigma_c\sigma_r + s\sigma_c\right)^{-} \qquad (10)$$

in which σ_θ is the circumferential stress, σ_r is the radial stress, σ_c is the uniaxial compressive strength of the intact rock material, and m and s are the Hoek-Brown constants that depend on the properties of the rock mass and the extent to which it was broken before being subjected to the failure stresses σ_θ and σ_r.

For the plastic zone, the above equation is given as:

$$\sigma_\theta - \sigma_r = \left(m_g\sigma_r\sigma_c + s_g\sigma_c^{\,2}\right)^{\frac{1}{2}} \qquad (11)$$

where m_g and s_g are the Hoek-Brown constants for the plastic zone and vary as a function of the softening parameter γ^p.

In contrast to the solution presented by Brown et al. [1], the solution proposed in this work considers the elastic strains induced in the plastic zone. The relationships between the elastic strains ε_r^e, and ε_θ^e, and the stresses σ_r and σ_θ are given by Hooke's law [17]:

$$\varepsilon_r^e = \frac{1+\nu}{E_g}\left[(1-\nu)(\sigma_r-\sigma_0)+\nu(\sigma_\theta-\sigma_0)\right] \qquad (12)$$

$$\varepsilon_\theta^e = \frac{1+\nu}{E_g}\left[(1-\nu)(\sigma_\theta-\sigma_0)+\nu(\sigma_r-\sigma_0)\right] \qquad (13)$$

where σ_0 is the initial stress, and calculating from Eq. (4), E_g and ν are the elasticity modulus and the Poisson's ratio of the rock mass, respectively. However, for the plastic zone, the elasticity modulus E_g varies as a function of the softening parameter γ^p.

It should be noted that in the plastic zone, the failure and dilation parameters, appearing in Eqs. (9) and (11), and also the rock mass elastic modulus appearing in Eqs. (12) and (13), can be described by a bilinear function based on the deviatoric plastic strain γ^p:

$$\omega = \begin{cases} \omega_i - (\omega_i - \omega_r)\dfrac{\gamma^p}{\gamma^{p^\star}} & 0 < \gamma^p < \gamma^{p^\star} \\ \omega_r & \gamma^p \geq \gamma^{p^\star} \end{cases} \qquad (14)$$

where ω represents one of the parameters m_g, s_g, ψ_g and E_g, and $\gamma^{p^\star}$ is the critical deviatoric plastic strain from

which the residual behavior starts, and should be identified by experiments. The subscripts '*i*' and '*r*' denote the initial and residual values, respectively.

4 ANALYSIS OF THE PLASTIC ZONE

For both cases (the horizontal and the vertical directions) a plastic zone of radius R_p will be formed around the tunnel. The governing equations on the plastic zone are similar, but not identical, for both cases.

It is important to highlight that the strains and stresses in the plastic zone depend on two factors: on a physical variable *r*, which is the distance to the centre of the excavation; and on a fictitious 'time' variable $\tau = R_p$, which is a measure of the plasticity evolution. In this regard, the dimensionless variable ρ is considered, that maps the physical plane (r, τ) into a plane of coordinate ρ according to the following transformation (see Fig. 6):

$$\rho = \frac{r}{\tau} \quad \text{or} \quad \rho = \frac{r}{R_p} \qquad (15)$$

Based on the above transformation, the solutions for the strain and stress fields do not depend on the plastic radius.

In this regard, the equilibrium Eq. (3) can be expressed with respect to the normalized radius $\rho = \frac{r}{R_p}$ as:

$$\frac{d\sigma_r}{d\rho} - \frac{\sigma_\theta - \sigma_r}{\rho} + F_r R_p = 0 \qquad (16)$$

where F_r is the radial body force. F_r is equal to $-\gamma$ for the vertical direction, and it is equal to zero for the horizontal direction (see Fig. 5).

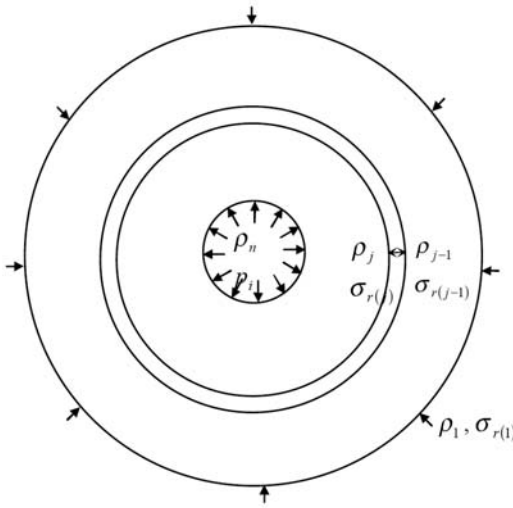

Figure 6. Normalized plastic zone with a finite number of annular elements.

A combination of the failure criterion, i.e., Eq. (11), and equilibrium equation, i.e., Eq. (16), gives:

$$\frac{d\sigma_r}{d\rho} + F_r R_p = \frac{\left(m_g \sigma_r \sigma_c + s_g {\sigma_c}^2\right)^{\frac{1}{2}}}{\rho} \qquad (17)$$

It is assumed that in the plastic zone the total strains consist of the elastic and plastic parts:

$$\varepsilon_r = \varepsilon_r^e + \varepsilon_r^p, \quad \varepsilon_\theta = \varepsilon_\theta^e + \varepsilon_\theta^p \qquad (18)$$

where ε_r and ε_θ are total radial and circumferential strains, respectively, and the superscripts e and p denote the elastic and plastic parts of the strains, respectively.

Thus, the total strain rates $\dot{\varepsilon}_\theta$ and $\dot{\varepsilon}_r$ can be written in terms of the elastic $\left(\dot{\varepsilon}_\theta^e, \dot{\varepsilon}_r^e\right)$ and plastic $\left(\dot{\varepsilon}_\theta^p, \dot{\varepsilon}_r^p\right)$ components as:

$$\dot{\varepsilon}_r = \dot{\varepsilon}_r^e + \dot{\varepsilon}_r^p, \quad \dot{\varepsilon}_\theta = \dot{\varepsilon}_\theta^e + \dot{\varepsilon}_\theta^p \qquad (19)$$

where the dot denotes the derivative of strain with respect to the fictitious time variable $\tau = R_p$ ($\dot{\varepsilon} = \frac{\partial \varepsilon}{\partial \tau}$), and ε_r^e and ε_θ^e are obtained using Hooke's law, i.e., Eqs. (12) and (13).

For the Mohr–Coulomb type of plastic potential function (8), elimination of the plastic multiplier $\dot{\lambda}$ from the flow rule, i.e., equations (6) and (7), gives the relation between the plastic parts of the radial and circumferential strain rates as follows:

$$\dot{\varepsilon}_r^p + K_\Psi \dot{\varepsilon}_\theta^p = 0 \qquad (20)$$

where the coefficient of dilation K_ψ is obtained from Eq. (9).

Based on the given transformation (Eq. (15)), the partial derivatives of the field functions with respect to the variables r and $\tau = R_p$ are evaluated with the operators:

$$\frac{\partial(\ )}{\partial r} = \frac{1}{R_p}\frac{\partial(\ )}{\partial \rho} \qquad (21)$$

$$\frac{\partial(\ )}{\partial \tau} = -\frac{\rho}{R_p}\frac{\partial(\ )}{\partial \rho} \qquad (22)$$

Eliminating u_r from Eqs. (5) by applying Eqs. (15) and (21) develops the simple compatibility equation:

$$\varepsilon_r = \rho \varepsilon_\theta' + \varepsilon_\theta \qquad (23)$$

where ε' is defined as:

$$\varepsilon' = \frac{d\varepsilon}{d\rho} \qquad (24)$$

Since a multi-linear behavior model and the incremental theory of plasticity have been used, the governing equa-

tions on the stresses and strains in the plastic zone have no analytical solutions, and must be solved numerically, as presented in Appendix A.

Defining the stresses and strains on the outer boundary of the plastic zone, where $\rho = \rho_1 = 1$, successive values of the stresses and strains are calculated from the formulations presented in Appendix A by successive increments of ρ_j (see Fig. 6) until the value of the radial stress for a specific ρ_n (i.e. $\sigma_{r(n)}$) reaches p_i .

Thus, for an analysis of the plastic zone it is necessary to calculate the boundary stresses at the external radius of the plastic zone (plastic radius) by considering the interactions between the elastic and plastic zones.

5 ANALYSIS OF THE ELASTIC ZONE

It should be noted that the tunnel excavation induces additional stresses on the rock mass initially subjected to equal field stresses; thus, the final stresses in the rock mass will be equal to the sum of the initial stresses and the induced stresses.

As the excavation is taking place, the stresses $\delta\sigma_\theta$ and $\delta\sigma_r$ are induced in the rock mass. By reducing the initial portion of the stresses from equilibrium Eq. (3), the governing equilibrium equation in terms of the induced stresses $\delta\sigma_r$ and $\delta\sigma_\theta$ is given by:

$$\frac{d\delta\sigma_r}{dr} - \frac{(\delta\sigma_\theta - \delta\sigma_r)}{r} = 0 \qquad (25)$$

In the elastic zone, Hooke's law for plane-strain conditions can be used between the induced stresses and strains [17]:

$$\delta\sigma_r = \frac{E_0}{(1+\nu)(1-2\nu)}\left[(1-\nu)\varepsilon_r + \nu\varepsilon_\theta\right] \qquad (26)$$

$$\delta\sigma_\theta = \frac{E_0}{(1+\nu)(1-2\nu)}\left[(1-\nu)\varepsilon_\theta + \nu\varepsilon_r\right] \qquad (27)$$

A combination of the equilibrium equation (25) with the above equations (Eqs. (26) and (27)); and then applying the strain-displacement Eqs. (5), gives the following equation for the unknown radial displacement u_r:

$$-\frac{u_r}{r^2} + \frac{1}{r}\frac{du_r}{dr} + \frac{d^2u_r}{dr^2} = 0 \qquad (27)$$

This differential equation has an analytical solution for the elastic zone by applying the boundary conditions at the internal and external radii. The boundary conditions are different for both cases (the horizontal and vertical directions) (see Fig 5), and thus the corresponding analytical formulations will be different.

For the case of the horizontal direction:

$$\delta\varepsilon_{r(r)} = -\delta\varepsilon_{\theta(r)} = \frac{1+\nu}{E_0}\delta\sigma_{r(R_p)}\frac{R_p^2}{r^2} \qquad (28)$$

$$\delta\sigma_{r(r)} = -\delta\sigma_{\theta(r)} = \delta\sigma_{r(R_p)}\frac{R_p^2}{r^2} \qquad (29)$$

For the case of vertical direction:

$$\delta\sigma_{r(r)} = -\delta\sigma_{r(R_p)}\frac{R_p^2}{h_0^2 - R_p^2}\left(1 - \frac{h_0^2}{r^2}\right) \qquad (30)$$

$$\delta\sigma_{\theta(r)} = -\delta\sigma_{r(R_p)}\frac{R_p^2}{h_0^2 - R_p^2}\left(1 + \frac{h_0^2}{r^2}\right) \qquad (31)$$

$$\delta\varepsilon_{\theta(r)} = -\frac{1+\nu}{E_0}\delta\sigma_{r(R_p)}\frac{R_p^2}{h_0^2 - R_p^2}\left(1 - 2\nu + \frac{h_0^2}{r^2}\right) \qquad (32)$$

$$\delta\varepsilon_{r(r)} = -\frac{1+\nu}{E_0}\delta\sigma_{r(R_p)}\frac{R_p^2}{h_0^2 - R_p^2}\left(1 - 2\nu - \frac{h_0^2}{r^2}\right) \qquad (33)$$

Based on the above equations, the same expressions for the induced stresses and strains are obtained, for both cases (the horizontal and the vertical directions), for a deep tunnel, namely where $h_0 \gg R_p$. On the other hand, it is observed that the gravitational loads will not affect the displacements in the elastic zone directly.

In the above equations, $\delta\sigma_{r(R_p)}$ is the induced radial stress at the plastic radius, and is obtained from:

$$\delta\sigma_{r(R_p)} = \sigma_{r(R_p)} - \sigma_{r0(R_p)} \qquad (34)$$

The final stresses ($\sigma_{r(r)}$, $\sigma_{\theta(r)}$), at any radius in the elastic zone, are obtained from the sum of the initial portions ($\sigma_{r0(r)}$, $\sigma_{\theta0(r)}$) and the induced portions ($\delta\sigma_{r(r)}$, $\delta\sigma_{\theta(r)}$).

$$\sigma_{r(r)} = \sigma_{r0(r)} + \delta\sigma_{r(r)} \qquad (35)$$

$$\sigma_{\theta(r)} = \sigma_{\theta0(r)} + \delta\sigma_{\theta(r)} \qquad (36)$$

The final radial and circumferential stresses at the plastic radius ($\sigma_{\theta(R_p)}$ and $\sigma_{r(R_p)}$) must satisfy the strength criterion; therefore, substituting these stresses into the Hoek–Brown strength criterion (i.e., Eq. (10)), and solving the equation obtained, gives the final boundary radial stress at the plastic radius $\sigma_{r(R_p)}$.

For the vertical direction:

$$\sigma_{r(R_p)} = \frac{1}{2}\left(m_i\sigma_c + 2\beta(1+\alpha)\right) - \left(m_i^2\sigma_c^2 + 4m_i\beta\sigma_c(1+\alpha) + 4\alpha s_i\sigma_c^2\left(2 + \alpha + \frac{1}{\alpha}\right)\right)^{\frac{1}{2}} \qquad (37)$$

$$\alpha = \frac{R_p^2}{h_0^2 - R_p^2}\left(1 + \frac{h_0^2}{R_p^2}\right) \qquad (38)$$

$$\beta = (1+\alpha)\sigma_{0\left(R_p,\theta=90^\circ\right)} \qquad (39)$$

And for the horizontal direction:

$$\sigma_{r\left(R_p\right)} = \frac{1}{2}\left(\lambda - \sqrt{\lambda^2 + 4\lambda\sigma_{0\left(\theta=0^\circ\right)} + s_i\sigma_c^2}\right) + \sigma_{0\left(\theta=0^\circ\right)} \quad (40)$$

$$\lambda = \frac{\left(m_i\sigma_c\right)}{4} \qquad (41)$$

Where m_i and s_i are the failure parameters for the original rock mass.

It should be noted that the plastic zone around the circular opening is only formed when the internal support pressure p_i is lower than a critical value of $\sigma_{r(R_p=r_i)}$ (where $R_p = r_i$).

As mentioned, for deep tunnels, $h_0 \gg r_0$, the governing equations in the elastic zone for both the horizontal and vertical directions are identical. However, in this case, the weight of the plastic zone may be significant; and thus the gravitational loads must be taken into account.

6 COMPUTATION PROCEDURE

As illustrated in Appendix A, in the plastic zone, the finite-difference calculations are carried out in terms of the normalized radius $\rho = \frac{r}{R_p}$. First, the boundary stresses and strains at the plastic radius (ρ_1=1 or r_1=R_p) are calculated from the equations presented in Section 5. Then, the successive values of the stresses and strains in the plastic zone are computed from the equations presented in Appendix A. The computations of the stresses $\sigma_{r(j)}$ and $\sigma_{\theta(j)}$ and the strains $\varepsilon_{r(j)}$ and $\varepsilon_{\theta(j)}$ are carried out until the equilibrium conditions at the tunnel radius are satisfied. Thus, when the value of radial stress, for a specific ρ_n, satisfies equation $\sigma_{r(j)}$=p_i, the computations will be stopped. The new value of the plastic radius will then be obtained, by dividing the tunnel radius r_i by this final value of ρ_n.

When the value of the plastic radius R_p is not initially determined, the computations must be performed iteratively. Thus, the value of plastic radius R_p, obtained in each step, is used for computations of the subsequent step.

7 ILLUSTRATIVE EXAMPLES

The solution described in this paper has been programmed in the FORTRAN language for use with a computer. This program was used to analyze several typical tunnels, and the results were then interpreted.

EXAMPLE 1

In this example the same tunnel as in Brown et al. [1] and Sharan [2] was analyzed, and the results were then compared. In Brown et al.'s, and Sharan's closed-form solutions, an elastic brittle rock mass behavior model has been used. Brown et al. neglected the elastic strain distribution in the plastic zone, while Sharan utilized an approximate formula for the elastic strains. In the proposed method, the analyses were performed for two values of γ^{p^*}, i.e., γ^{p^*}= 0 (corresponding to a brittle behavior) and γ^{p^*}= 0.01 (corresponding to a strain-softening behavior).

A typical deep tunnel, $h_0 \gg r_0$, with the following typical properties is considered:

m_i = 1.7, m_r = 1, s_i = 0.0039, s_r = 0, σ_c = 30 MPa,

ν = 0.25, $E_0 = E_r$ = 5500 Mpa, γ = 0.028 MN/m^3,

σ_0 = 30 MPa, r_i = 5 m, p_i = 5 MPa, $\psi_i = 30^\circ$, $\psi_r = 20^\circ$

where E_0 and E_r are the elastic modulus for the original and residual rock masses, respectively, and ψ_i and ψ_r are the dilation angles for the original and residual rock masses, respectively.

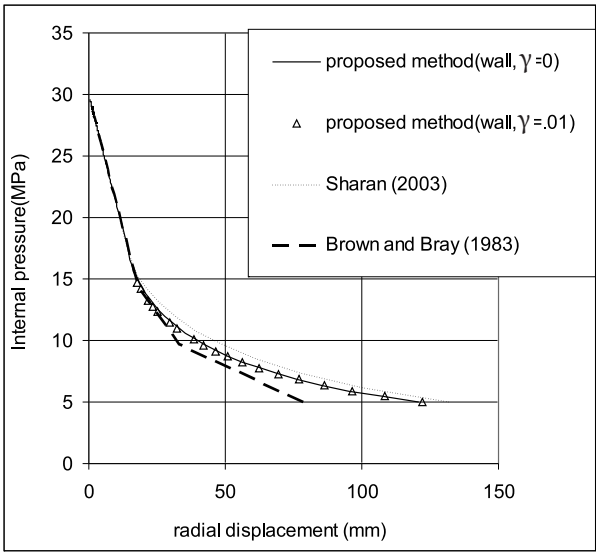

Figure 7. Ground-response curves for the tunnel of the example 1.

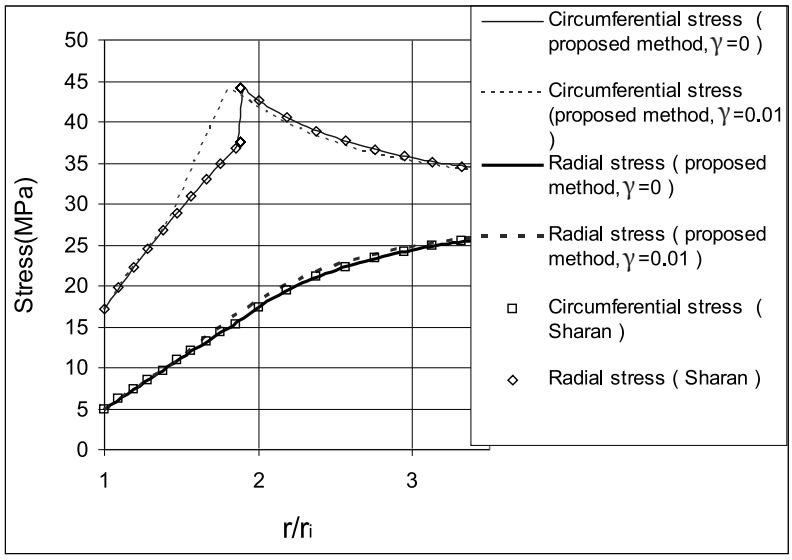

Figure 8. Distribution of stresses around the tunnel of example 1.

As this case is a deep tunnel, only the formulations for the horizontal direction are utilized.

Figs. 8 and 9 show the ground-response curves and the stress distributions obtained from the three theoretical methods. It is observed that Sharan's approximation overestimates the displacements, while Brown et al.'s approximation underestimates the displacements, as illustrated by Lee and Pietruszczak [6]. Furthermore, in the proposed method, the strain-softening behavior can also be considered, and as shown in Figs. 8 and 9, for $\gamma^{p^*} = 0.01$, the ground-response curves coincide, while the plastic radii are different.

EXAMPLE 2

In this example, the effect of gravitational loads being applied in the plastic zone is examined. In addition, the proposed method is compared with a numerical method.

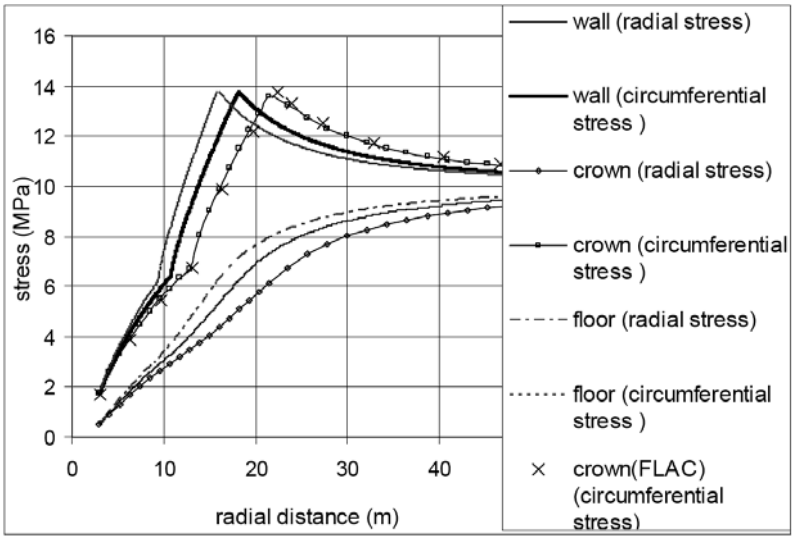

Figure 9. Distribution of stresses around the tunnel of example 2.

The following data set is used:

$$\gamma^{p^*} = 0.004,\ m_i = 0.3,\ m_r = 0.1,\ s_i = 0.0001,\ s_r = 0,$$

$$\sigma_c = 30 \text{ MPa},\ \psi_i = \psi_r = 0,\ \nu = 0.25,\ E_0 = 10000 \text{ MPa},$$

$$E_r = 4000 \text{ MPa},\ \gamma = 0.028 \text{ MN/m}^3,\ p_s = 0 \text{ MPa},$$

$$\sigma_0 = 10 \text{ MPa},\ r_i = 3 \text{ m},\ p_i = 0.5 \text{ MPa}$$

This tunnel is also a deep tunnel; thus, for the analysis of the elastic zone the formulations proposed for the horizontal direction are utilized. However, because of the effect of gravitational loads in the plastic zone the results for the horizontal and vertical directions can be different.

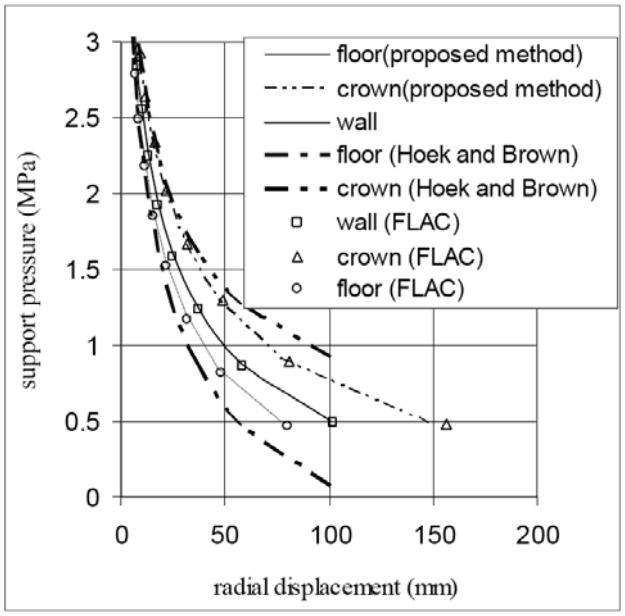

Figure 10. The ground-response curves for the tunnel of example 2.

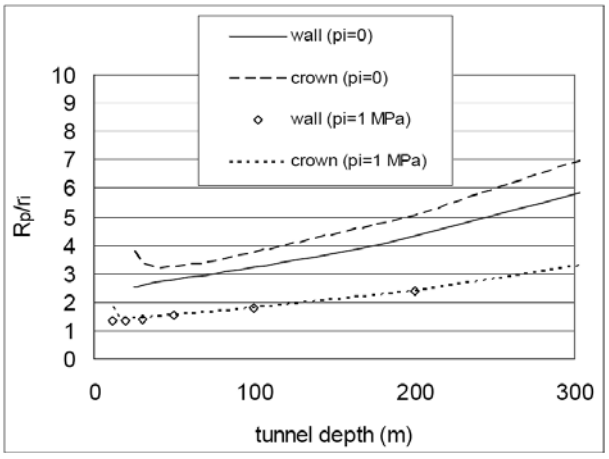

Figure 11. Variation of the plastic radius versus h_0.

In Figs. 10 and 11 the ground-response curves and the stress distribution through the horizontal and vertical directions are depicted. In these figures, the results obtained from the FLAC 2D program [20] are also plotted, which show a very proper agreement with the proposed solution.

Fig. 9 shows that due to the weight of the plastic zone, the plastic radii are not the same for the different directions, and the plastic radius increases from the floor to the crown.

In Fig. 10, the ground-response curves obtained from Hoek and Brown's [19] simplified method are also plotted. As is clear from this figure, Hoek and Brown's method overestimates the tunnel convergence for the crown, and underestimates it for the floor.

EXAMPLE 3

In this example, the effect of tunnel depth and horizontal and vertical directions on the results are examined. For this purpose, the following data set is used:

$$\gamma^{p^*} = 0.0,\ m_i = 0.7,\ m_r = 0.3,\ s_i = 0.001,\ s_r = 0,$$

$$\sigma_c = 30 \text{ MPa},\ \psi_i = \psi_r = 0,\ \nu = 0.25,\ E_0 = 1500 \text{ MPa},$$

$$E_r = 1500 \text{ MPa},\ \gamma = 0.028 \text{ MN/m}^3,\ p_s = 5.0 \text{ MPa},$$

$$r_i = 5 \text{ m},\ p_i = 0.0 \text{ MPa and } 1.0 \text{ MPa}$$

Fig. 11, shows the variations of the plastic radii for different values of the tunnel depth, for two cases of $p_i = 0.0$ MPa and 1.0 MPa. In the case of $p_i = 0.0$ MPa, the plastic deformations in the plastic zone are large enough, and so the effect of gravitational loads is significant. Consequently, the plastic radii, through the horizontal and vertical directions, are not the same. On the other hand, in the case of $p_i = 1.0$ MPa , the deformations in the plastic zone are small; thus, the plastic radii, through the horizontal and vertical directions, are approximately the same. It is concluded that the plastic radius for the tunnel crown is larger than the tunnel wall, and the difference increases with the increasing the depth of the tunnel.

The values of the radial displacements at the distance $r = h_0$ along the horizontal and vertical directions may be utilized as the lower-bound and the upper-bound values, respectively, for approximating the surface settlement. In Fig. 12 the radial displacements at the distance $r = h_0$ for different values of h_0 for two cases of $p_i = 0.0$ MPa and 1.0 MPa were plotted. It is clear that at small values of h_0, because of the short distances between the ground surface and the plastic zone, excessive surface

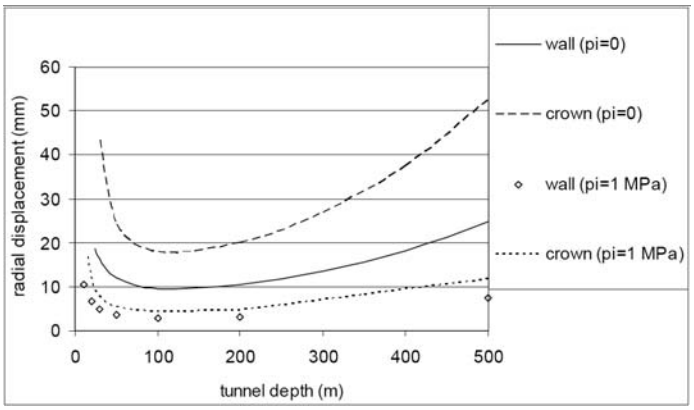

Figure 12. Variations of radial displacement at $r = h_0$ versus h_0 .

settlements occur. On the other hand, at large values of h_0, the surface settlement may increase with depth due to an increase in magnitude of the in-situ stresses.

Furthermore, in Fig. 12, it is clear that the displacements through the tunnel crown are larger than the tunnel wall, and the difference becomes greater for the wider plastic zones.

8 CONCLUSIONS

In order to examine the C.-C. method, commonly used for the analysis of tunnels, and to demonstrate the effect of the classic assumptions on the characteristics of the ground-response curve, an analytical solution was proposed.

The solution is relatively simple, easy to use, and can readily indicate its sensitivity through a range of possible ground parameters, boundary conditions, and applied loads.

In this solution, the formulations were derived through horizontal and vertical directions, by taking the gravitational loads into account. It was shown that, for practical cases even for shallow tunnels, the convergence–confinement method is reasonably applicable. However, the effect of gravitational loads in the analyses can be noticeable, and ignoring the plastic load can lead to large errors in the calculations.

REFERENCES

[1] Brown, E.T., Bray, J.W., Ladanyi, B., Hoek, E. (1983). Ground response curves for rock tunnels. *Journal of geotechnical Engineerin*, Vol. 109, No. 1, pp. 15–39.

[2] Sharan, S.K. (2003). Elastic–brittle–plastic analysis of circular openings in Hoek–Brown media. *Int. J. Rock Mech. Min. Sci.*, Vol. 40, No.6, pp. 817–824.

[3] Carranza-Torres, C., Fairhurst, C. (1999). The elasto-plastic response of underground excavations in rock masses that satisfy the Hoek–Brown failure criterion. *Int. J. Rock Mech. Min. Sci.*, Vol. 36, No. 6, pp. 777–809.

[4] Park, K.-H., Kim, Y.-J. (2006). Analytical solution for a circular opening in, an elasto-brittle-plastic rock. *Int. J. Rock Mech. Min. Sci*., Vol. 43, pp. 616–622.

[5] Guan, Z., Jiang, Y., Tanabasi, Y., (2007). Ground reaction analyses in conventional tunneling excavation. *Tunnelling and Underground Space Technology*, Vol. 22, No. 2, pp. 230–237.

[6] Lee, Y.-K., Pietruszczak, S. (2008). A new numerical procedure for elasto-plastic analysis of a circular opening excavated in a strain-softening rock mass. *Tunnelling and Underground Space Technology*, Vol. 23, No. 5, pp. 588–599.

[7] Fahimifar, A., Zareifard, M.R. (2009). A theoretical solution for analysis of tunnels below groundwater considering the hydraulic– mechanical coupling. *Tunnelling and Underground Space Technology*, Vol. 24, No. 6, pp. 634–646.

[8] Carranza-Torres, C., Fairhurst, C. (2000). Application the convergence-confinement method of tunnel design to rock masses that satisfy the Hoek–Brown failure criterion. *Tunnelling and Underground Space Technology*, Vol. 16, No. 2, pp. 187–213.

[9] González-Nicieza C, Álvarez-Vigil A.E., Menéndez-Díaz A., González-Palacio C. (2008). Influence of the depth and shape of a tunnel in the application the convergence-confinement method. *Tunnelling and Underground Space Technology*, Vol. 23, No. 1, pp. 25–37.

[10] Lu A-Z., Xu G-s., Sun, F., Sun, W. (2010). Elasto-plastic analysis of a circular tunnel including the effect of the axial in situ stress. *Int. J. Rock Mech. And Mining Sci*., Vol. 47, No. 1, pp. 50–59.
[11] Detournay, E. and Fairhurst, C. (1987). Two-dimensional elastoplastic analysis of along, cylindrical cavity under non-hydrostatic loading. *Int. J. Rock Mech. Min. Sci. & Geomech. Abstr.*, Vol. 24, No. 4, pp. 197–211.
[12] Reed MB. (1988) . The influence of out-of-plane stress on a plane strain problem in rock mechanics. *Int. J. Numer Anal Meth Geomech*., Vol. 12, No., pp 173–81.
[13] Hoek E., Brown E.T. (1980). Underground excavations in rock. The Institute of Mining and Metallurgy, London
[14] Carranza-Torres, C. and Fairhurst, C. (1997). On the stability of tunnels under gravity loading, with post-peak softening of the ground. *Int. J. Rock Mech. Min. Sci*., Vol. 34, No. 3-4, pp. 75.e1–75.e18.
[15] Fahimifar, A., Zareifard, M.R., (2010). The elasto-plastic response of circular tunnel considering gravity loads for two cases of plane strain and plane stress conditions. Geotechnical Chalenges in Megacites, Moscow. V. 2.
[16] Kolymbas D. (2005). Tunnelling and Tunnel Mechanics. Springer-Verlag, Berlin Heidelberg (2)
[17] Timoshenko S.P., and Goodier J.N. (1982). Theory of Elasticity. McGraw-Hill, New York
[18] Alonso, E., Alejano, L.R., Varas, F., Fdez-Manin, G., Carranza-Torres, C. (2003). Ground response curves for rock masses exhibiting strain-softening behaviour. *Int. J. Numer. Anal. Meth. Geomech*., Vol. 27, No. 13, pp. 1153– 1185.
[19] Hoek E., Brown E.T. (1980). Underground excavations in rock. The Institute of Mining and Metallurgy, London
[20] Itasca. (2000). User manual for FLAC, Version 4.0. Itasca Consulting Group Inc.: Minnesota

APPENDIX A. STRESS AND STRAIN ANALYSES FOR THE PLASTIC ZONE

stress analysis

The finite-difference method (FDM) is used to solve Eq. (17) for $\sigma_{r(j)}$ and $\sigma_{\theta(j)}$ by selecting an annular element of the outer radius ρ_{j-1} and the inner radius ρ_j shown in Fig. 6:

$$\sigma_{r(j)} = \sigma_{r(j-1)} + \lambda_1 - \left\{\lambda_2 + \lambda_3 \sigma_{r(j-1)}\right\}^{\frac{1}{2}} \qquad \text{(A1)}$$

where:

$$\overline{m}_g = \frac{m_{g(j)} + m_{g(j)}}{2} \qquad \text{(A2)}$$

$$\overline{s}_g = \frac{s_{g(j)} + s_{g(j)}}{2} \qquad \text{(A3)}$$

$$\lambda_1 = F_r R_p \left(\rho_j - \rho_{j-1}\right) + 2\overline{m}_g \sigma_c \left(\frac{\rho_j - \rho_{j-1}}{\rho_j + \rho_{j-1}}\right)^2 \qquad \text{(A4)}$$

$$\lambda_2 = \left(\frac{\rho_j - \rho_{j-1}}{\rho_j + \rho_{j-1}}\right)^2 \left[\overline{m}_g^2 \sigma_c^2 \left(\frac{\rho_j - \rho_{j-1}}{\rho_j + \rho_{j-1}}\right)^2 + 2\overline{m}_g \sigma_c F_r R_p \left(\rho_j - \rho_{j-1}\right) + 4\overline{s}_g \sigma_c^2\right] \qquad \text{(A5)}$$

$$\lambda_3 = 4\overline{m}_g \sigma_c \left(\frac{\rho_j - \rho_{j-1}}{\rho_j + \rho_{j-1}}\right)^2 \qquad \text{(A6)}$$

The failure criterion, i.e., Eq. (11), can then be used to calculate the corresponding values of $\sigma_{r(j)}$ as follows:

$$\sigma_{\theta(j)} = \sigma_{r(j)} + \left(m_{g(j)} \sigma_c \sigma_{r(j)} + s_{g(j)} \sigma_c^{\,2}\right)^{\frac{1}{2}} \qquad \text{(A7)}$$

$\sigma_{r(j)}$ is a function of the plastic radius R_p for vertical direction, as observed in Eq. (A1); thus, the analyses are carried out alternately in a sequence of successive approximations, to achieve the appropriate convergence of the plastic radius R_p.

strain analysis

The total strain rates ε'_θ and ε'_r can be written in terms of the elastic $\left(\varepsilon'^{e}_\theta, \varepsilon'^{e}_r\right)$ and plastic $\left(\varepsilon'^{p}_\theta, \varepsilon'^{p}_r\right)$ components as:

$$\varepsilon'_r = \varepsilon'^{e}_r + \varepsilon'^{p}_r \quad \varepsilon'_\theta = \varepsilon'^{e}_\theta + \varepsilon' \qquad \text{(A8)}$$

Considering the Mohr–Coulomb type of plastic potential function, i.e., Eq. (8), the elimination of the plastic multiplier $\dot{\lambda}$ from the flow rule, i.e., Eqs. (6) and (7), and using Eq. (15) gives the relation between the plastic parts of radial and circumferential strain rates:

$$\varepsilon'^{p}_r + K_\Psi \varepsilon'^{p}_\theta = 0 \qquad \text{(A9)}$$

The finite-difference method (FDM) is used to solve the governing differential equation obtained from Eqs (23) and (A9) for $\varepsilon'_{\theta(\rho_i)}$ and $\varepsilon'_{r(\rho_i)}$ by using the annular elements shown in Fig. 6 as:

$$\varepsilon'_{\theta(\rho_i)} = \frac{\left(2\overline{\Omega}_{(j)} - \varepsilon'_{\theta(j-1)}\left(3+\overline{K}_{\Psi(j)}\right)\right)\rho_{(j-1)} + \varepsilon'_{\theta(j-1)}\rho_j\left(1+\overline{K}_{\Psi(j)}\right) - 2\overline{\Omega}_{(j)}\rho_{(j)}}{\left(1+\overline{K}_{\Psi(j)}\right)\rho_{(j-1)} - \left(3+\overline{K}_{\Psi(j)}\right)\rho_{(j)}} \qquad \text{(A10)}$$

where:

$$\varepsilon'^{e}_{r(j)} = \frac{\varepsilon^{e}_{r(j)} - \varepsilon^{e}_{r(j-1)}}{\rho_{(j)} - \rho_{(j-1)}} \qquad \text{(A11)}$$

$$\varepsilon'^{e}_{\theta(\rho_i)} = \frac{\varepsilon^{e}_{\theta(j)} - \varepsilon^{e}_{\theta(j-1)}}{\rho_{(j)} - \rho_{(j-1)}} \qquad \text{(A12)}$$

$$\overline{K}_{\Psi(j)} = \frac{K_{\Psi(j)} + K_{\Psi(j-1)}}{2} \qquad \text{(A13)}$$

$$\Omega_{(j)} = \varepsilon'^{e}_{r(j)} + K_{\Psi(j)}\varepsilon'^{e}_{\theta(j)} \qquad \text{(A14)}$$

$$\overline{\Omega}_{(j)} = \frac{\Omega_{(j)} + \Omega_{(j-1)}}{2} \qquad \text{(A15)}$$

thus:

$$\varepsilon_{\theta(j)} = \varepsilon'_{\theta(j)}\left(\rho_{(j)} - \rho_{(j-1)}\right) + \varepsilon_{\theta(j-1)} \qquad \text{(A16)}$$

In addition, the corresponding values of the strains $\varepsilon^{e}_{r(j)}$, $\varepsilon^{e}_{\theta(j)}$, $\varepsilon^{p}_{r(j)}$, $\varepsilon^{p}_{\theta(j)}$, $\varepsilon_{r(j)}$ and $\varepsilon_{r(j)}$ are obtained using Eqs. (12), (13), (18), (A8), and (A9).

Using Eqs. (18) and (23), the following boundary conditions are obtained for the plastic radius, where, $\rho = \rho = 1$:

$$\varepsilon_{r(j=1)} = \varepsilon^{e}_{r(j=1)} \quad \textit{and} \quad \varepsilon^{p}_{r(j=1)} = 0 \qquad \text{(A17)}$$

$$\varepsilon_{\theta(j=1)} = \varepsilon^{e}_{\theta(j=1)} \quad \textit{and} \quad \varepsilon^{p}_{\theta(j=1)} = 0 \qquad \text{(A18)}$$

$$\varepsilon'_{\theta(j=1)} = \varepsilon_{r(j=1)} - \varepsilon_{\theta(j=1)} \qquad \text{(A19)}$$

NOMENCLATURE:

E_0: Deformability modulus of elastic rock mass
E_g: Deformability modulus of plastic rock mass
h_0: Depth of the tunnel
F_r: Radial body force
F_θ: Circumferential body force
K: Lateral stress coefficient
K_ψ: Dilation factor
m_i,s_i: Material constants for original rock mass.
m_r,s_r: Material constants for residual rock mass
m_g,s_g: Material constants for broken rock mass
p_s: Surcharge load
r: Radial distance from the center of the tunnel
r_i: Tunnel radius
R_p: Radius of plastic zone
u_r: Radial displacement
(x,y,z): Cartesian coordinates
$\delta\sigma_\theta$: induced circumferential stress
$\delta\sigma_r$: induced radial stress
ε_1: Major Principal strain of rock mass
ε_3: Minor principal strain of rock mass
ε_θ: Circumferential strain
ε_r: Radial strain
ε^e_θ: Elastic circumferential strain
ε^e_r: Elastic radial strain
ε^p_θ: Plastic circumferential strain
ε^p_r: Plastic radial strain
$\dot{\varepsilon}$: Derivative of strain ε with respect to τ
ε': Derivative of strain ε with respect to ρ
γ: Unit weight of rock mass
γ^p: Deviatoric plastic strain
γ^{p^*}: Critical deviatoric plastic strain
η: Softening parameter.
$\dot{\lambda}$: Plastic multiplier
ν_r: Poisson's ratio of rock mass
θ: Angle measured clockwise from the horizontal direction
ρ: Normalized radius
σ_1: Major principal stress
σ_3: Minor principal stress
σ_c: Uniaxial compressive strength of intact rock
σ_θ: Circumferential stress
σ_r: Radial stress
$\sigma_{\theta 0}$: Initial circumferential stress
σ_{r0}: Initial radial stress
σ_0: Initial stress
τ: Fictitious time variable
ψ_i: Dilation angle for original rock mass
ψ_r: Dilation angle for residual rock mass
ψ_g: Dilation angle for plastic rock mass
Subscript *e*: Refers to elastic part
Subscript *p*: Refers to plastic part